



# Gold nanoparticle-loaded hollow Prussian Blue nanoparticles with peroxidase-like activity for colorimetric determination of L-lactic acid

Dandan Zhou<sup>1</sup> · Ke Zeng<sup>1</sup> · Minghui Yang<sup>1</sup>

Received: 20 December 2018 / Accepted: 27 December 2018 / Published online: 21 January 2019  
© Springer-Verlag GmbH Austria, part of Springer Nature 2019

## Abstract

The intrinsic peroxidase-like activity of hollow Prussian Blue nanoparticle-loaded with gold nanoparticles (Au@HMPB NPs) were applied to oxidize the substrate 3,3',5,5'-tetramethylbenzidine (TMB) in the presence of H<sub>2</sub>O<sub>2</sub> to give a blue-green coloration. The morphology of the Au@HMPB NPs and its peroxidase-mimicking activity was characterized in detail. The catalytic activity follows Michaelis-Menten kinetics and is higher than that of HMPB NPs not loaded with gold nanoparticles. The NPs were employed to detect L-lactic acid colorimetrically (at 450 nm) via detection of H<sub>2</sub>O<sub>2</sub> that is generated during enzymatic oxidation by L-lactate oxidase (LOx). The limit of detection is 4.2 μM. The assay was successfully applied to the quantitation of L-lactic acid in spiked human serum samples.

**Keywords** Tetramethylbenzidine · Human serum sample · Lactate oxidase · Gold nanoparticles

## Introduction

The detection of L-lactic acid is of great significance in bioanalytical and clinical fields. L-lactic acid is usually served as indicator for applications such as diagnosing heart disease and neonatology studies [1, 2]. Therefore, the development of low cost methods for L-lactic acid detection with high specificity and high sensitivity are highly required. Different methods for lactic acid detection have been reported [3, 4]. Most of these methods are based on the enzymatic reactions. For example, lactate dehydrogenase (LDH) can catalyze L-lactic acid in the presence of cofactor NAD<sup>+</sup> to generate pyruvic acid (PA) and NADH, which can be detected by absorption or fluorescence spectroscopy [5]. Alternatively, L-lactic acid can be detected by various amperometric biosensors based on the formation of H<sub>2</sub>O<sub>2</sub> via the oxidation of L-lactic

acid by L-lactate oxidase (LOx) [6]. Besides, enzyme-based colorimetric analysis is of highly competitive, as it can be detected by bare eyes and does not require complex and expensive instruments. In such colorimetric assays, chromogenic substrates were used to react with H<sub>2</sub>O<sub>2</sub> in the presence of horseradish peroxidase (HRP) to form colored products [7, 8].

The commonly used chromogenic substrates include 3,3',5,5'-tetramethylbenzidine (TMB) [9], 2,2'-azinobis(3-ethylbenzothiazoline-6-sulfonic acid) diammonium salt (ABTS) [10] and o-phenylenediamine (OPD) [11]. Among these substrates, TMB is a better choice since ABTS can be oxidized in the absence of peroxidase using H<sub>2</sub>O<sub>2</sub> alone [12]. HRP possess high efficiency and specificity under mild and eco-friendly conditions. However, its inherent defects are also apparent, such as high cost and easy of denaturation under harsh conditions. Thus, it is imperative to develop artificial enzymes to replace HRP.

Nanomaterial based artificial enzymes have aroused the attention of researchers. Since Fe<sub>3</sub>O<sub>4</sub> nanoparticles was found to exhibit intrinsic peroxidase-like activity [13], various nanomaterials have been evaluated to possess a peroxidase-like capacity, including Gold NPs [14], Co<sub>3</sub>O<sub>4</sub> NPs [15], V<sub>2</sub>O<sub>5</sub> nanowires [16], carbon nanomaterials [17] and ZnFe<sub>2</sub>O<sub>4</sub> NPs [18]. Since these nanomaterials with peroxidase-like activity have the advantages of low cost, ease of preparation and high stability compared to HRP, they can be extensively applied in biosensors and bioassays [19].

**Electronic supplementary material** The online version of this article (<https://doi.org/10.1007/s00604-018-3214-7>) contains supplementary material, which is available to authorized users.

✉ Minghui Yang  
yangminghui@csu.edu.cn

<sup>1</sup> Key Laboratory of Hunan Province for Water Environment and Agriculture Product Safety, College of Chemistry and Chemical Engineering, Central South University, Changsha 410083, China

Prussian Blue nanoparticles (PB NPs) possess high peroxidase-like activity, which is widely used in electrochemistry [20, 21]. Little attention has been paid to the peroxidase mimicking behavior of PB NPs for colorimetric biosensing [22]. However, the intrinsic blue color of PB NPs can interfere with the colorimetric detection while the poor dispersibility of PB NPs in aqueous solutions has been reported to inhibit its catalytic activity [23]. To overcome these defects, Wang et al. reported filling of multi-walled carbon nanotubes with PB nanoparticles as peroxidase mimic for colorimetric sensing of  $\text{H}_2\text{O}_2$  and glucose, which not only improved the color distribution and dispersibility of PB NPs but also enhanced the peroxidase-like activity of PB NPs. [24]

Here, we report on gold nanoparticle-loaded hollow mesoporous Prussian Blue nanoparticles (Au@HMPB NPs) as peroxidase mimic for colorimetric determination of L-lactic acid in serum. The loading of gold nanoparticles onto the surface of PB NPs not only prevented the aggregation of PB nanoparticles, but also enhanced its peroxidase-like activity [25–27]. The detection of L-lactic acid was achieved through the detection of  $\text{H}_2\text{O}_2$  generated by LOx catalyzed oxidation of L-lactic acid.

## Experimental section

### Chemical and materials

Unless otherwise stated, the reagents and chemicals used in this study were of analytical grade. Polyvinylpyrrolidone (PVP), potassium ferricyanide ( $\text{K}_3[\text{Fe}(\text{CN})_6]$ ), L-lactic acid and L-lactate oxidase (LOx) were obtained from Sigma-Aldrich (<https://www.sigmaaldrich.com/>). 3,3',5,5'-Tetramethylbenzidine (TMB) were obtained from Heowns Co., Ltd. (Tianjin, China, <http://www.heowns.cn/>). Gold (III) chloride tetrahydrate ( $\text{HAuCl}_4 \cdot 4\text{H}_2\text{O}$ ) were purchased from Sangon Bitech Co., Ltd. (Shanghai, China, <https://www.sangon.com/>).

Transmission electron microscope (TEM) images of Au@HMPB were obtained from FEI Tecnai G2 60–300 microscopy (Hillsboro, USA). The optical densities measurements were carried out using a Biotek Model ELx800 Microplate Reader (Shanghai, China).

### Synthesis of hollow mesoporous Prussian Blue (HMPB) nanoparticles

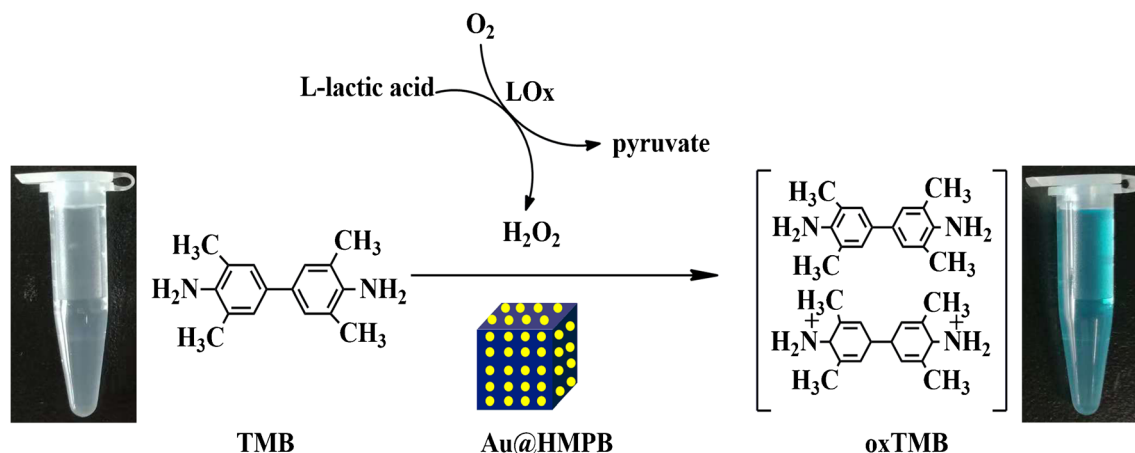
HMPB nanoparticles were prepared according to previous reports with minor revisions [28]. The detailed synthesis procedures are shown in electronic supporting material.

### Synthesis of Au@HMPB nanoparticles

Briefly,  $5 \text{ mg} \cdot \text{mL}^{-1}$  HMPB nanoparticles (1 mL) and 0.01% chlorauric acid ( $\text{HAuCl}_4$ ) solution (16 mL) were mixed and heated. After boiling, 1% sodium citrate solution (0.34 mL) was quickly added into the above solution under vigorous stirring for 5 min in the dark. The final product was washed and collected by successive centrifugation.

### Peroxidase-like activity assays

In a typical assay, the peroxidase-like activity of HMPB NPs and Au@HMPB NPs were carried out at  $40^\circ\text{C}$  in 0.2 M sodium acetate buffer (pH 3.5) in the presence of  $800 \mu\text{M}$  freshly prepared TMB (TMB dissolved in DMSO) and  $400 \text{ mM}$   $\text{H}_2\text{O}_2$ . The kinetic analysis with  $\text{H}_2\text{O}_2$  as the substrate was carried out using standard reaction condition (described above) by varying the concentration of  $\text{H}_2\text{O}_2$  (0–0.5 M) at a fixed concentration of TMB ( $800 \mu\text{M}$ ). Similarly, the kinetic analysis with TMB as the substrate was performed using above method by varying the concentration of TMB (0–1 mM) with  $400 \text{ mM}$   $\text{H}_2\text{O}_2$ .



**Scheme 1** Schematic representation for the detection of L-lactic acid

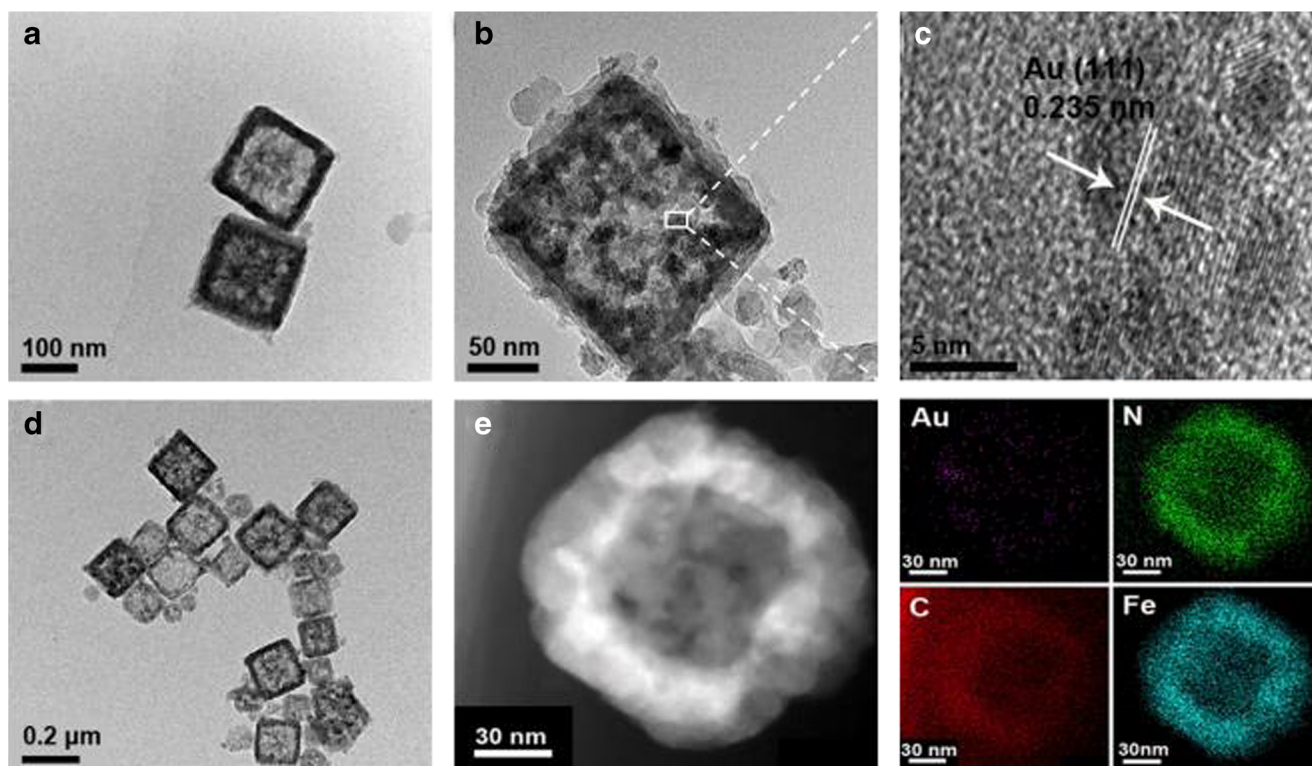


**Fig. 1** TEM image of **a** HMPB NPs, **b** Au@HMPB NPs, **c** HRTEM image, **d** dispersed Au@HMPB NPs and **e** elemental mapping images of Au@HMPB NPs (C, N, Fe, Au)

### Detection of L-lactic acid by Au@HMPB NPs

50  $\mu\text{L}$  of 0.01  $\text{mg}\cdot\text{mL}^{-1}$  LOx, 400  $\mu\text{L}$  of L-lactic acid with different concentrations and 50  $\mu\text{L}$  of 200 mM phosphate buffer (pH 7.0) were mixed and incubated at 37  $^{\circ}\text{C}$  for 10 min. Then 90  $\mu\text{L}$  of the above mixture, 100  $\mu\text{L}$  freshly prepared TMB substrate solution (800  $\mu\text{M}$  TMB in 0.2 M acetate buffer, pH 3.5), and 10  $\mu\text{L}$  of the Au@HMPB NPs (0.04  $\text{mg}\cdot\text{mL}^{-1}$ ) were added into the well of 96-well plate and incubated at 40  $^{\circ}\text{C}$  for 1 h in the dark. The color change was visually observed. After adding 4.0  $\mu\text{L}$  of stop solution (2.0 M  $\text{H}_2\text{SO}_4$ ), the absorbance was recorded at 450 nm with the ELx800 microplate reader.

### Determination of L-lactic acid in serum

For L-lactic acid analysis in serum samples, a standard addition experiment was performed. The serum sample was diluted by phosphate buffer (pH 7.0, 200 mM), spiked with different concentration of L-lactic acid and then analyzed.

## Results and discussion

### Choice of materials

Gold nanoparticles were loaded onto HMPB to enhance the catalytic activity of HMPB as gold nanoparticles also have

peroxidase mimicking behavior. The hollow structure of Au@HMPB NPs can increase surface area that leads to more active sites, which is beneficial for peroxidase-like activity of Au@HMPB NPs.

### Synthesis and characterization of Au@HMPB and HMPB nanoparticles

Scheme 1 shows the schematic representation for the detection of L-lactic acid. The HMPB is synthesized by

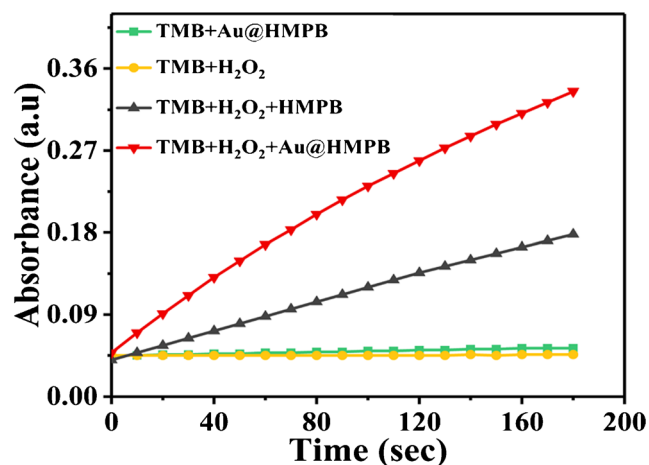
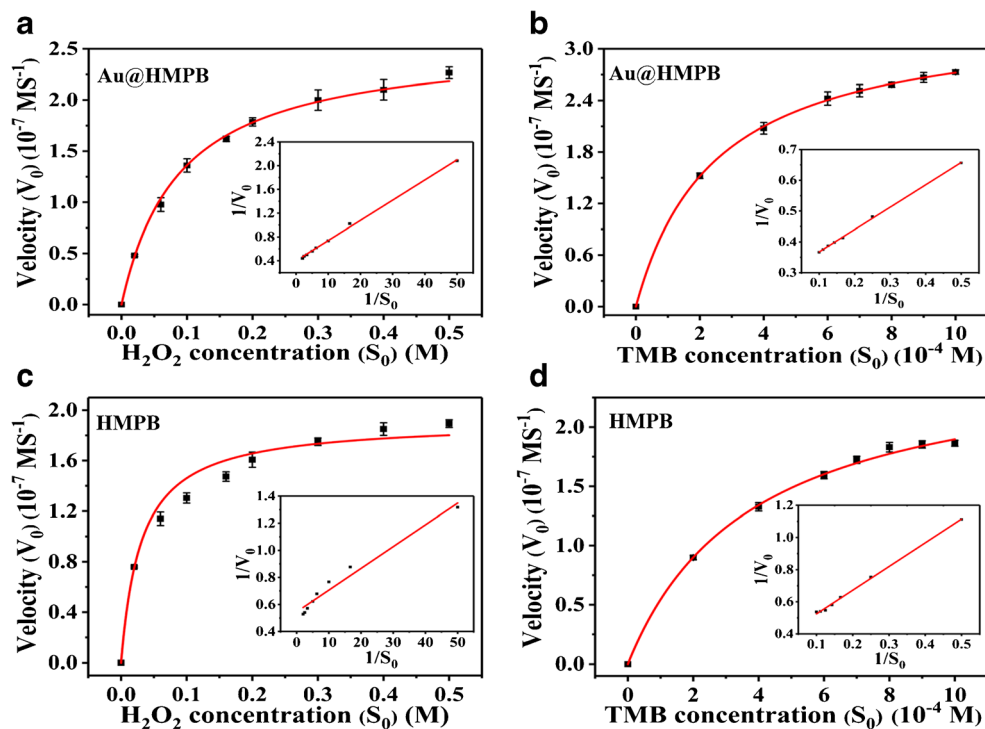


**Fig. 2** UV-vis absorption-time curve of the TMB- $\text{H}_2\text{O}_2$  system under different conditions

**Fig. 3** Steady-state kinetic study using the Michaelis–Menten model and Lineweaver–Burk model (insets) for Au@HMPB and HMPB NPs by **a**, **c** varying the concentration of  $\text{H}_2\text{O}_2$  with a fixed amount of TMB and **b**, **d** varying the concentration of TMB with a fixed amount of  $\text{H}_2\text{O}_2$



etching solid PB with acid, and the gold nanoparticles are loaded onto HMPB by reducing  $\text{HAuCl}_4$  with sodium citrate. The morphology of the Au@HMPB and HMPB nanoparticles were characterized by transmission electron microscope (TEM). As shown in Fig. 1a, the unmodified HMPB possess a hollow and highly porous structure with an average size of 150 nm. The nanoporous shell of the hollow particles resulted in an increase of the surface area, which is beneficial for the following growth of Au nanoparticles. After deposition of Au nanoparticles, Au nanoparticles were distributed on the surface of the nanoparticles (Fig. 1b). In the high-resolution TEM (HRTEM) image (Fig. 1c), the lattice spacing of gold layer was about 0.235 nm, which corresponds to the (111) facets of Au. The gold nanoparticles modified HMPB can be well dispersed into solution (Fig. 1d). Elemental mapping data further proved that Au nanoparticles were well-distributed over the entire HMPB nanoparticles (Fig. 1e).

**Table 1** The comparison of the kinetic parameters of HRP, HMPB and Au@HMPB NPs

Materials	Substrate	Km/mM	Vmax/ $10^{-6}\text{MS}^{-1}$	Temperature
Au@HMPB	TMB	0.25	0.34	40 °C
	$\text{H}_2\text{O}_2$	88.72	0.25	
HMPB	TMB	0.38	0.26	
	$\text{H}_2\text{O}_2$	30.93	0.19	
HRP	TMB	0.43	0.10	
	$\text{H}_2\text{O}_2$	3.70	0.08	

#### Peroxidase-mimetic activity of Au@HMPB and HMPB NPs

To compare the peroxidase enzyme mimetic activity of HMPB and Au@HMPB NPs, TMB was chosen as the substrate. As shown in Fig. 2, HMPB and Au@HMPB can both catalyze oxidation of TMB in the presence of  $\text{H}_2\text{O}_2$  to produce the blue color complex, similar to HRP. In the absence of HMPB or Au@HMPB NPs, there was no change in the color of solution, suggesting that the oxidation of TMB would not happen. What's more, it can be seen from the Fig. 2 that the catalytic rate of Au@HMPB NPs is higher than that of HMPB NPs,

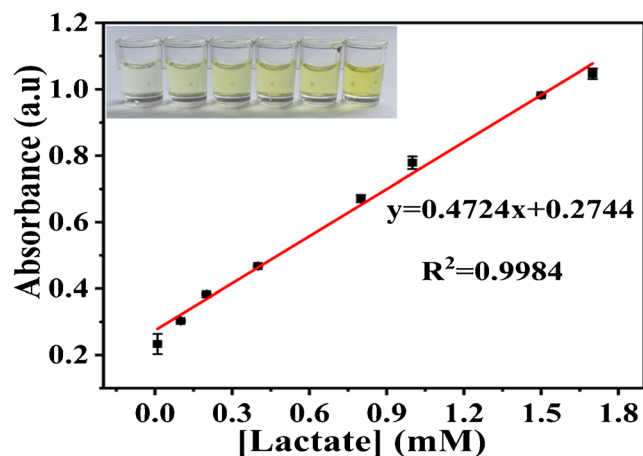


**Fig. 4** Linear calibration plot for L-lactic acid assay by the combination of L-lactic acid oxidation catalyzed by LOx and TMB oxidation catalyzed by Au@HMPB NPs. Absorption Data acquired at 450 nm was utilized to draw the calibration curve



**Table 2** Compare the performance of the assay for L-lactic acid detection with previous reports

Analytical method	Biosensing materials	Detection limit ( $\mu\text{M}$ )	Linear range ( $\mu\text{M}$ )	Reference
Electrochemistry	N-CNTs/LOx	4.1	$14\text{--}3.25 \times 10^2$	[4]
Fluorimetry	Al-coated nanoprobe/LDH	20	$60\text{--}1 \times 10^3$	[32]
Fluorimetry	CuONPs/LDH	0.045	0.8~80	[33]
Chemiluminescent	Luminol/LOx	9.2	$50\text{--}4 \times 10^3$	[34]
Colorimetry	Au-Ag/LOx	0.33	0.1~22, 22~220	[35]
Colorimetry	Au@HMPB/LOx	4.2	$10\text{--}1.7 \times 10^3$	This work

CNT represents carbon nanotube

suggesting that Au@HMPB NPs exhibit higher peroxidase-like activity. The enhanced catalytic activity is mainly ascribed to the loaded Au nanoparticles.

### Optimization of method

The following parameters were optimized: (a) Sample pH value and (b) reaction temperature. Respective data and Figures are given in the Electronic Supporting Material. The following experimental conditions were found to give best results: (a) Best sample pH value of 3.5 and (b) optimal reaction temperature of 40 °C.

**Steady-state kinetic analysis of Au@HMPB and HMPB NPs** The peroxidase-like activity of Au@HMPB and HMPB NPs were also studied by Michaelis-Menten curves, which were obtained by varying the concentration of  $\text{H}_2\text{O}_2$  and TMB (Fig. 3). Michaelis-Menten constant ( $K_m$ ) and maximal velocity ( $V_{\text{max}}$ ), as the crucial enzyme kinetic parameters, can be obtained by fitting the data to Lineweaver-Burk double-reciprocal plot (inset of Fig. 3).  $K_m$  is an indicator of enzyme affinity toward its substrates [29]. A high  $K_m$  indicates weak affinity, whereas a low value suggests high affinity. The  $K_m$  value for Au@HMPB NPs towards TMB is lower than that of HRP and HMPB,

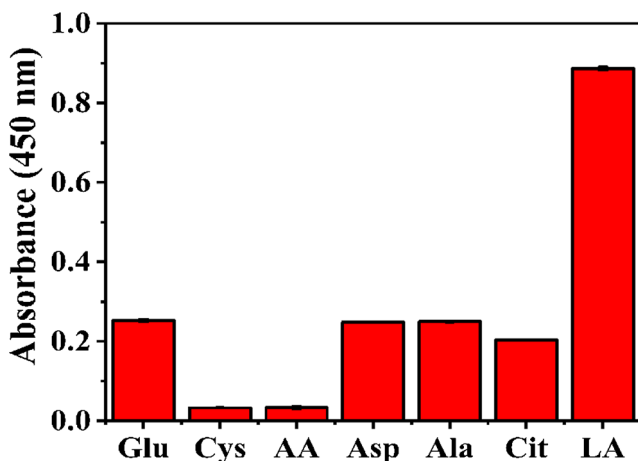


**Fig. 5** Selectivity of the L-lactic acid assay. Glucose, L-cysteine ascorbic acid, L-aspartic acid, L-alanine, citric acid and L-lactic acid (each 1 mM) were tested

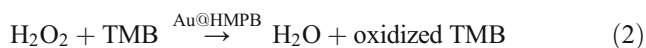
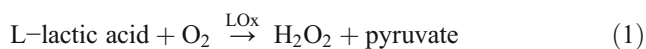
suggesting that Au@HMPB NPs have higher affinity with TMB in comparison to HRP and HMPB NPs. Moreover, the  $K_m$  value of HMPB NPs is also lower than that of HRP. However, the  $K_m$  value of Au@HMPB NPs with  $\text{H}_2\text{O}_2$  was higher than that for HRP, indicating that a higher  $\text{H}_2\text{O}_2$  concentration was required to achieve maximal activity for the Au@HMPB NPs (Table 1) [13, 30]. The surface area is closely related to the catalytic active site [31]. Therefore, the hollow and multihole structure of Au@HMPB NPs can expose more active sites that enhanced the peroxidase mimicking behavior. Moreover, Au NPs also has peroxidase-like activities [26], which indicated that the observed enhanced activity of Au@HMPB NPs can be attributed to the synergistic effect between Au NPs and HMPB NPs. A similar phenomenon was also reported for graphene oxide-AuNCs and Au@Ag heterogeneous NRs [25–27].

### Analytical application

Reliable and sensitive detection of L-lactic acid is of great importance in biochemistry, clinical diagnostics and food industry. In this assay, LOx catalyzed the L-lactic acid to generate  $\text{H}_2\text{O}_2$  and pyruvate. Then,  $\text{H}_2\text{O}_2$  can react with TMB in the presence of Au@HMPB NPs. Therefore, the detection of L-lactic acid can be achieved via detection of enzymatic byproduct,  $\text{H}_2\text{O}_2$  (Eqs. 1 and 2). As shown in Fig. 4, the colorimetric responses increase linearly with the increasing concentration of L-lactic acid. The linear range for L-lactic acid detection is 10–1700  $\mu\text{M}$  with the linear regression equation of  $y = 0.4724x + 0.2744$  and correlation coefficient ( $R^2$ ) of 0.998. The detection limit is calculated to be 4.2  $\mu\text{M}$  based on  $S/N = 3$ .

**Table 3** Analytical results of L-lactic acid determination in human serum

L-lactic acid added (mM)	Found (mM)	Recovery (%)	RSD (%)
0.1	0.098	98.0	2.3
0.4	0.411	102.8	1.1
0.8	0.825	103.1	1.0
1	1.03	103.3	2.4
1.7	1.67	98.2	0.34



The analytical performance of the assay is compared with previous literature reports for L-lactic acid detection. From Table 2, it can be seen the performance of our assay is comparable or better than literature reports.

To investigate the specificity of our assay, a series of controlled experiments were conducted using glucose (Glu), L-cysteine (Cys), ascorbic acid (AA), L-aspartic acid (Aap), L-alanine (Ala) and citric acid (Cit) instead of L-lactic acid. As shown in Fig. 5, no significant signals were observed for the control experiments, suggesting that LOx has high substrate specificity. The result also demonstrated that Au@HMPB NPs as peroxidase mimetics were sensitive and specific enough to detect L-lactic acid.

To evaluate the feasibility of our study for analysis of L-lactic acid in biological samples, a standard addition method was applied to the detection of L-lactic acid in human serum samples. As shown in Table 3, the recoveries of the different concentration of L-lactic acid in serum samples ranging from 98.0% to 103.3% and the relative standard deviation (RSD) was estimated to be <5%. Thus the Au@HMPB NPs were promising as peroxidase mimetics for potential application of L-lactic acid detection clinically.

## Conclusions

We demonstrate here that both Au@HMPB and HMPB NPs possess high peroxidase-like activity that can oxidize TMB in the presence of H<sub>2</sub>O<sub>2</sub>. Moreover, Au@HMPB NPs exhibit higher catalytic activity and higher stability in aqueous solution than HMPB NPs. The enhanced peroxidase-like activity is mainly due to the large surface area and the synergistic effect between Au NPs and HMPB NPs. Taking into account the above factors, Au@HMPB NPs were chosen to detect L-lactic acid via the detection of H<sub>2</sub>O<sub>2</sub> that generated by LOx catalyzed oxidation of L-lactic acid. The synthesized Au@HMPB NPs may find wide applications as peroxidase mimic in different areas. However, the assay was based on detection of absorption intensity of oxidized TMB product. If the enzyme-mimicking nanomaterials can oxidize substrate to generate fluorescence emission, the detection sensitivity can be significantly enhanced.

**Acknowledgments** The authors thank the support of this work by the National Natural Science Foundation of China (No. 21575165).

**Compliance with ethical standards** The author(s) declare that they have no competing interests.

**Publisher's Note** Springer Nature remains neutral with regard to jurisdictional claims in published maps and institutional affiliations.

## References

1. Stacpoole PW, Wright EC, Baumgartner TG, Bersin RM, Buchalter S, Curry SH, Duncan CA, Harman EM, Henderson GN, Jenkinson S, Lachin JM, Lorenz A, Schneider SH, Siegel JH, Sumner WR, Thompson D, Wolfe CL, Zorovich B (1992) A controlled clinical trial of dichloroacetate for treatment of lactic acidosis in adults. *N Engl J Med* 327(22):1564–1569
2. Broder G, Weil MH (1964) Excess lactate: an index of reversibility of shock in human patients. *Science* 143(3613):1457–1459
3. Tumang CA, Borges EP, Reis BF (2001) Multicommutation flow system for spectrophotometric l(+)-lactate determination in silage material using an enzymatic reaction. *Anal Chim Acta* 438(1):59–65
4. Goran JM, Lyon JL, Stevenson KJ (2011) Amperometric detection of l-lactate using nitrogen-doped carbon nanotubes modified with lactate oxidase. *Anal Chem* 83(21):8123–8129
5. Brand A, Singer K, Koehl Gudrun E, Kolitzus M, Schoenhammer G, Thiel A, Matos C, Bruss C, Klobuch S, Peter K, Kastenberger M, Bogdan C, Schleicher U, Mackensen A, Ullrich E, Fichtner-Feigl S, Kesselring R, Mack M, Ritter U, Schmid M, Blank C, Dettmer K et al (2016) LDHA-associated lactic acid production blunts tumor immunosurveillance by T and NK cells. *Cell Metab* 24(5):657–671
6. Romero MR, Ahumada F, Garay F, Baruzzi AM (2010) Amperometric biosensor for direct blood lactate detection. *Anal Chem* 82(13):5568–5572
7. He Y, Niu X, Shi L, Zhao H, Li X, Zhang W, Pan J, Zhang X, Yan Y, Lan M (2017) Photometric determination of free cholesterol via cholesterol oxidase and carbon nanotube supported Prussian blue as a peroxidase mimic. *Microchim Acta* 184(7):2181–2189
8. Qu F, Li T, Yang M (2011) Colorimetric platform for visual detection of cancer biomarker based on intrinsic peroxidase activity of graphene oxide. *Biosens Bioelectron* 26(9):3927–3931
9. Li W, Chen B, Zhang H, Sun Y, Wang J, Zhang J, Fu Y (2015) BSA-stabilized Pt nanozyme for peroxidase mimetics and its application on colorimetric detection of mercury(II) ions. *Biosens Bioelectron* 66:251–258
10. Kim MI, Shim J, Li T, Lee J, Park HG (2011) Fabrication of nanoporous nanocomposites entrapping Fe<sub>3</sub>O<sub>4</sub> magnetic nanoparticles and oxidases for colorimetric biosensing. *Chem Eur J* 17(38):10700–10707
11. Guan J, Peng J, Jin X (2015) Synthesis of copper sulfide nanorods as peroxidase mimics for the colorimetric detection of hydrogen peroxide. *Anal Methods* 7(13):5454–5461
12. Chu BH, Kang BS, Ren F, Chang CY, Wang YL, Pearton SJ, Glushakov AV, Dennis DM, Johnson JW, Rajagopal P, Roberts JC, Piner EL, Linthicum KJ (2008) Enzyme-based lactic acid detection using AlGaIn GaN high electron mobility transistors with ZnO nanorods grown on the gate region. *Appl Phys Lett* 93(4):042114
13. Gao L, Zhuang J, Nie L, Zhang J, Zhang Y, Gu N, Wang T, Feng J, Yang D, Perrett S, Yan X (2007) Intrinsic peroxidase-like activity of ferromagnetic nanoparticles. *Nat Nanotechnol* 2:577–583
14. Jv Y, Li B, Cao R (2010) Positively-charged gold nanoparticles as peroxidase mimic and their application in hydrogen peroxide and glucose detection. *Chem Commun* 46(42):8017–8019
15. Mu J, Wang Y, Zhao M, Zhang L (2012) Intrinsic peroxidase-like activity and catalase-like activity of Co<sub>3</sub>O<sub>4</sub> nanoparticles. *Chem Commun* 48(19):2540–2542
16. André R, Natálio F, Humanes M, Leppin J, Heinze K, Wever R, Schröder H-C, Müller WEG, Tremel W (2011) V<sub>2</sub>O<sub>5</sub> nanowires with an intrinsic peroxidase-like activity. *Adv Funct Mater* 21(3):501–509

17. Tian J, Liu Q, Asiri AM, Qusti AH, Al-Youbi AO, Sun X (2013) Ultrathin graphitic carbon nitride nanosheets: a novel peroxidase mimetic, Fe doping-mediated catalytic performance enhancement and application to rapid, highly sensitive optical detection of glucose. *Nanoscale* 5(23):11604–11609
18. Su L, Feng J, Zhou X, Ren C, Li H, Chen X (2012) Colorimetric detection of urine glucose based ZnFe<sub>2</sub>O<sub>4</sub> magnetic nanoparticles. *Anal Chem* 84(13):5753–5758
19. Nasir M, Nawaz MH, Latif U, Yaqub M, Hayat A, Rahim A (2017) An overview on enzyme-mimicking nanomaterials for use in electrochemical and optical assays. *Microchim Acta* 184(2):323–342
20. Zhang W, Ma D, Du J (2014) Prussian blue nanoparticles as peroxidase mimetics for sensitive colorimetric detection of hydrogen peroxide and glucose. *Talanta* 120:362–367
21. Zeng K, Yang M, Liu Y-N, Rasooly A (2018) Dual function hollow structured mesoporous Prussian blue mesocrystals for glucose biosensors. *Anal Methods* 10(32):3951–3957
22. Su L, Xiong Y, Yang H, Zhang P, Ye F (2016) Prussian blue nanoparticles encapsulated inside a metal–organic framework via in situ growth as promising peroxidase mimetics for enzyme inhibitor screening. *J Mater Chem B* 4(1):128–134
23. Michopoulos A, Kouloumpis A, Gournis D, Prodromidis MI (2014) Performance of layer-by-layer deposited low dimensional building blocks of graphene-Prussian blue onto graphite screen-printed electrodes as sensors for hydrogen peroxide. *Electrochim Acta* 146:477–484
24. Wang T, Fu Y, Chai L, Chao L, Bu L, Meng Y, Chen C, Ma M, Xie Q, Yao S (2014) Filling carbon nanotubes with Prussian blue nanoparticles of high peroxidase-like catalytic activity for colorimetric chemo- and biosensing. *Chem Eur J* 20(9):2623–2630
25. Han L, Li C, Zhang T, Lang Q, Liu A (2015) Au@Ag heterogeneous nanorods as nanozyme interfaces with peroxidase-like activity and their application for one-pot analysis of glucose at nearly neutral pH. *ACS Appl Mater Interfaces* 7(26):14463–14470
26. Lee Y, Garcia MA, Frey Huls NA, Sun S (2010) Synthetic tuning of the catalytic properties of Au-Fe<sub>3</sub>O<sub>4</sub> nanoparticles. *Angew Chem* 122(7):1293–1296
27. Tao Y, Lin Y, Huang Z, Ren J, Qu X (2013) Incorporating graphene oxide and gold nanoclusters: a synergistic catalyst with surprisingly high peroxidase-like activity over a broad pH range and its application for cancer cell detection. *Adv Mater* 25(18):2594–2599
28. Ming H, Shuhei F, Ryo O, Hiroaki S, Yoshihiro N, Julien R, Susumu K, Yusuke Y (2012) Synthesis of Prussian blue nanoparticles with a hollow interior by controlled chemical etching. *Angew Chem* 124(4):1008–1012
29. Kim M-C, Lee D, Jeong SH, Lee S-Y, Kang E (2016) Nanodiamond-gold nanocomposites with the peroxidase-like oxidative catalytic activity. *ACS Appl Mater Interfaces* 8(50):34317–34326
30. Liu M, Zhao H, Chen S, Yu H, Quan X (2012) Interface engineering catalytic graphene for smart colorimetric biosensing. *ACS Nano* 6(4):3142–3151
31. Komkova MA, Karyakina EE, Karyakin AA (2018) Catalytically synthesized Prussian blue nanoparticles defeating natural enzyme peroxidase. *J Am Chem Soc* 140(36):11302–11307
32. Zheng XT, Yang HB, Li CM (2010) Optical detection of single cell lactate release for cancer metabolic analysis. *Anal Chem* 82(12):5082–5087
33. Hu A-L, Liu Y-H, Deng H-H, Hong G-L, Liu A-L, Lin X-H, Xia X-H, Chen W (2014) Fluorescent hydrogen peroxide sensor based on cupric oxide nanoparticles and its application for glucose and l-lactate detection. *Biosens Bioelectron* 61:374–378
34. Ballesta-Claver J, Valencia-Mirón MC, Capitán-Vallvey LF (2008) One-shot lactate chemiluminescent biosensor. *Anal Chim Acta* 629(1):136–144
35. Zhang L, Hou W, Lu Q, Liu M, Chen C, Zhang Y, Yao S (2016) Colorimetric detection of hydrogen peroxide and lactate based on the etching of the carbon based Au-Ag bimetallic nanocomposite synthesized by carbon dots as the reductant and stabilizer. *Anal Chim Acta* 947:23–31